STUDY AND DESIGN OF (COMPARISON) 3-Z NETWORK BOOST CONVERTERS FOR RENEWABLE POWER SYSTEMS

Kiran Babu
M.Tech student, NSSCE Palakkad, kiranbabuenassery@gmail.com
Dr. Devi V
Professor, EEE department, NSSCE Palakkad, devinsspkd@gmail.com

Abstract: A converter that can reach a high voltage gain with fewer diodes and a small duty cycle (smaller than 33 percentage), meanwhile avoid my instability caused by saturation of its inductors is a 3-Z network. Conventional boost converters can realize high voltage gains at large duty cycles (normally exceeding 50 percentage) resulting in saturation of inductors. It also fulfils the stringent requirements from industry, particularly renewable power systems, to boost low voltage from clean sources such as photovoltaic (PV) arrays and fuel cells to high voltages for grid-connected converters. Here in this paper a detailed comparison of two types of 3-Z network boost converters are done with proper design and its continuous conduction modes is analyzed for different states of its components. It is then followed with the parameters design. Simulations and experiments are conducted to validate the effectiveness of the proposed converters.

Keywords: Boost converter, Continuous-conduction modes (CCMs), Discontinuous-current modes (DCMs), High-gain voltage.

I. INTRODUCTION

New industries based on renewable energy are unprecedentedly flourishing and have higher demands on the power electronics technology. For instance, renewable power systems require DC-DC boost converters to boost low voltages as back-up energy conversion for uninterruptible power systems. Highly efficient and high step-up DC-DC converters are necessary to handle large input current and sustain high output voltage. Theoretically speaking, the conventional boost converters can realize infinite voltage gain with an extreme duty cycle when ignoring parasitic parameters. Moreover, the conventional boost converters are restricted by the parasitic parameters of their components and suffer serious power loss. Furthermore, the modern semiconductor technology can still not provide efficient and economic high-voltage stress diodes and switches for the boost converters. In practical applications, the voltage gain of the conventional boost converters can maximally reach five to six times of the input voltage, which is far away from the practical requests.

To obtain the desired voltage, boost converters can be connected in series, which is, however, very complicated due to the additional switches and control units. Quadratic boost converters are the most popular cascaded converters applied in practice, in which two switches and control circuits are excessively used, but cannot ensure sufficient voltage gains. Further, many improvements based on the cascading techniques have been made, i.e., a cascade Cockcroft Walton voltage multiplier applied to a transformer less DC-DC converter, a high voltage-boosting converter based on bootstrap capacitors and boost inductors, a quadratic power converter, and different kinds of interleaved high step-up converters for reducing the current ripple and getting a high voltage gain. However, those proposals suffer from the problems of using multiple switches and control units, which increase the complexity and cost of the systems and reduce their sufficiency and reliability.

Some converters can reach high voltage gain by only one or two switches, e.g., a DC-DC multilevel boost converter and a switched-capacitor-based active-network converter, but the voltage gain is still not large enough for industrial applications. The voltage gains of the Z-source converters may be still not enough for many industrial applications, which puts forward a challenge for designing converters with even higher voltage gains.

A novel boost converter with three active Z-networks is proposed and thus named 3-Z-network converters, which not only have the advantages of the Z-network converters but also can reach much higher voltage gains. Moreover, the 3-Z-network converters operate not only in continuous conduction modes (CCMs) but also in discontinuous conduction modes (DCMs). CCM refers to the normal load condition, under which the traditional boost converters work. Due to the unstable energy source in renewable energy systems, such the PV systems, the load conditions become abnormal, corresponding to DCM.

II. 3-Z-NETWORK BOOST CONVERTERS

As shown in Figure.1 and Figure.2 the designs distinct features are not only to use just a single switch, but also the minimum number of diodes in both the converters. Moreover, the proposed converters can realize a higher voltage gain with a smaller duty cycle. The Figure.1 represents the 3-Z-network converter with two capacitors in the middle link. The Figure.2 represents the 3-Z-network converter with one diode and one capacitors in the middle link. Both the boost converters can operate in Continuous Conduction Mode (CCM) and Discontinuous conduction Mode (DCM). There are cases of DCM in terms of the discontinuous currents of inductors L_1, L_2, L_3 and L_4.

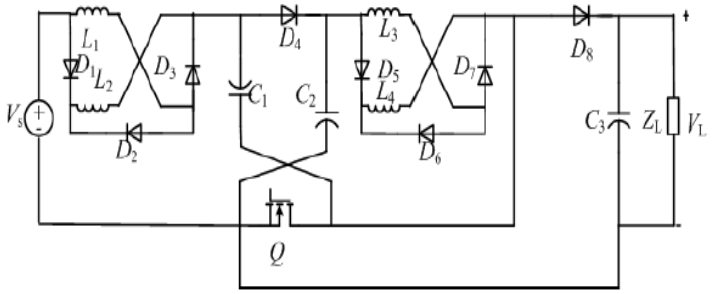

Figure.1 The proposed DC-DC 3-Z-network boost converter with capacitors in the middle link. (converter-1)

As CCM is normally employed in industrial applications, the operation of the proposed converters is analyzed in the sequel for this mode, only. For simplicity, it is assumed that all components are ideal, the freewheeling diode of the switch is ignored, the capacitances of the capacitors C_1; C_2; C_3 are large enough to consider the voltages Vc_1 ; Vc_2 ;Vc_3 to be constant as well as L_1= L_2 and L_3 = L_4.

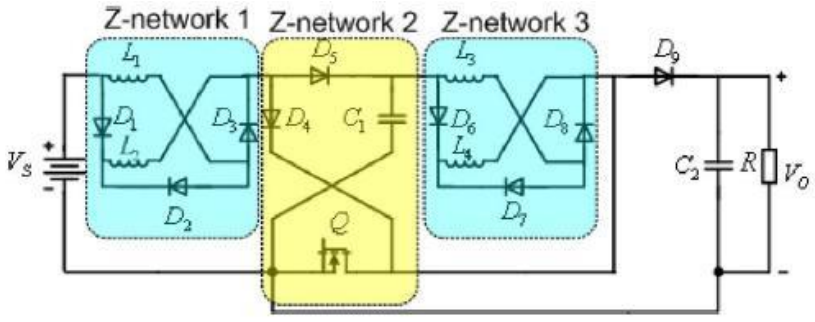

Figure.2 The proposed DC-DC 3-Z-network boost converter with one diode and one capacitors in the middle link.(converter-2)

Both the converters have the same working principle but had a difference in their gain. Converter-1 has a gain of 13 times the output voltage and converter-2 has 9 times the output voltage.

III. OPERATING PRINCIPLE

The 3-Z-network boost converters can operate both in CCM and DCM.

A) Continuous Current Modes [CCM]

For simplicity, it is assumed that ;

1) all the components are ideal,

2) the free-wheeling diode of the switch is ignored, and

3) $L_1 = L_2$ and $L_3 = L_4$

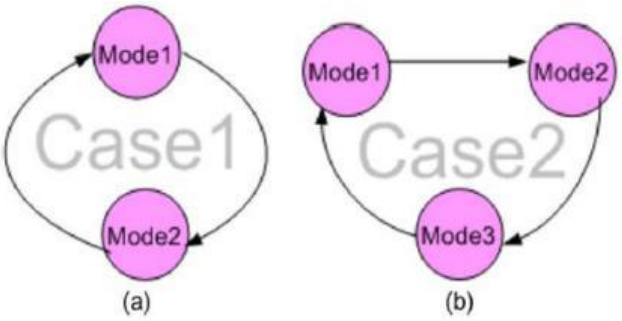

Figure 3 : Transitions between modes in CCM.

The inductors can have continuous or discontinuous currents under some combinations of the inductances, the load, and the duty cycle. Therefore, the proposed converter can function in the CCM or the DCM, which then correspond to six modes, i.e., six linear equivalent circuits, respectively. There in, V_{L1} ,V_{L2} , V_{L3}, and V_{L4} are voltages of L_1, L_2, L_3 and L_4, respectively. Assume the clockwise direction as positive directions of the reference currents, and the arrows shown in Figure 3 refer to the positive directions of the inductor reference voltages.

Moreover, the detailed states of the components in the circuit are shown in TABLE - I. Here, the proposed converter performance in CCMs are seen through Mode 1, Mode 2, Mode 3 shown in Figure 3.

B) Discontinuous Current Modes [DCM]

Here, the performance of the proposed converter DCM are given through Mode 1, Mode 2, Mode 3, Mode 4, Mode 5, Mode 6 shown in Figure 4.

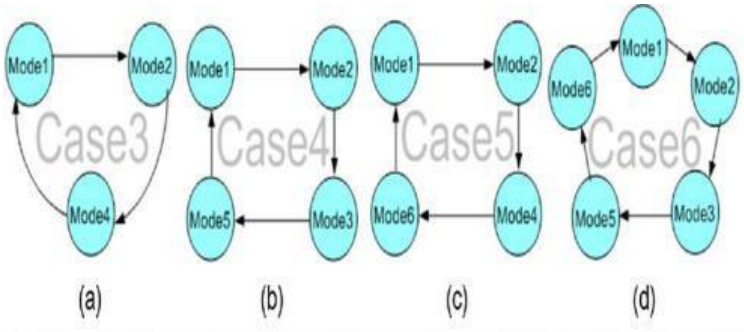

Figure.4 : Transitions between modes in DCM.

And the corresponding states of the components are shown in Table I.

TABLE I
Voltage stress of each semiconductor component in CCM

	Mode 1	Mode2
Q	on	off
D_1&D_3	on	off
D_2	off	on
D_4	off	on
D_5	on	off
D_6&D_8	off	on
D_7	on	off

IV. ANALYSIS OF EQUIVALENT CIRCUIT OF BOTH THE CONVERTERS
(During continuous conduction modes [CCM])

1) Converter-1 (3-Z-network boost converter with capacitors in the middle link)

There are two sub-modes of the converter in CCM, namely Mode 1 and 2, whose equivalent circuits are shown in Figure 2. Therein, V_{L1}, V_{L2}, V_{L3}, V_{L4}, are the voltages at L_1, L_2, L_3 and L_4, respectively.

Assume the clockwise direction as the reference current direction and the voltages marked in Figure 2 are regarded as the reference voltages of inductors. Denote with D the duty cycle of the switching signal applied at switch Q, with t_0 the beginning of a period of this signal, with t_1 the transition instant from Mode 1 to Mode 2 and with $t_2 = T$ the periods end.

A) Mode 1: t - [t_0;t_1]

shown in Figure.4, there are three loops in the circuit, and the arrows in the circuit diagram refer to the current directions in each loop. As Q turns on, the diodes D_1 and D_3 assume positive voltages and turn on synchronously; meanwhile, D_2 bears negative voltage and turns off. Thereafter, L_1 and L_2 are connected in parallel and, then, cascaded with C_1, Q and Vs to form Loop 1. The source Vs discharges energy to $L_1$and L_2, then currents i_{L1} and i_{L2} increase, and L_1 and L_2 store the energy.

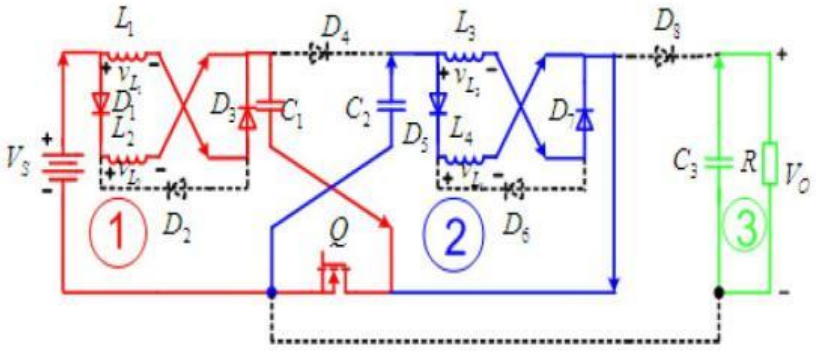

Figure.5 . Equivalent circuit- Mode 1

The waveforms of i_{L1} and i_{L2} are shown in Figure. 6(b), where $i_{L1} = i_{L2}$ due to the symmetrical structure of Z-network 1. Moreover, Loop 1 marked with red line in Mode 1, the voltages at L_1; L_2 can be obtained as,

$$V_{L1} = V_s - V_{c1}$$
$$V_{L2} = V_s - V_{c1}$$

where V_{L1}; V_{L2} and V_{C1} are the voltages at L_1; L_2 and C_1, respectively. In the meantime, D_4 and D_6 assume negative voltages and turn OFF, while D_5 and D_7 endure positive voltages and turn ON. Accordingly, L_3 and L_4 are connected in parallel and, then, cascaded with Q and C_2 to form Loop 2. The capacitor C_2 discharges its energy to L_3 and L_4, and currents i_{L3} and i_{L4} increase. Thus, L_3 and L_4 store energy. The waveforms of i_{L3} and i_{L4} are shown in Fig. 3.3(c), where $i_{L3} = i_{L4}$. Thus, according to Loop 2 marked with blue line in Mode 1, one has

$$V_{L3} = V_{C2}$$
$$V_{L4} = V_{C2}$$

where V_{L3} ; V_{L4} and V_{C2} are the voltages at L_3; L_4 and C_2, respectively. Meanwhile, D_8 assumes negative voltage and turns OFF, then capacitor C_3 and load Z_L are cascaded to form Loop 3. Here, C_3 discharges its energy to Z_L and the converters output voltage V_o is the voltage V_{C3} at capacitor C_3:

$$V_0 = V_{C3}$$

B) Mode 2: t - [t_1;t_2]

At instant t_1, Q turns OFF and the mode changes from Mode 1 to Mode 2, as shown in Fig. 4.2. As Q is off, D_1; D_3; D_5; D_7 assume negative voltages and turn OFF, whereas D_2; D_4; D_6 and D_8 turn ON and form three loops in this mode. Loop 1 marked with red line in Mode 2, discharges energy from Vs, L_1 and L_2 to C_2. Moreover, currents i_{L1} and i_{L2} decrease as shown in Figure. 6(b).

The analysis above can be expressed as

$$v_{L1} + v_{L2} = V_s - V_{C2}$$

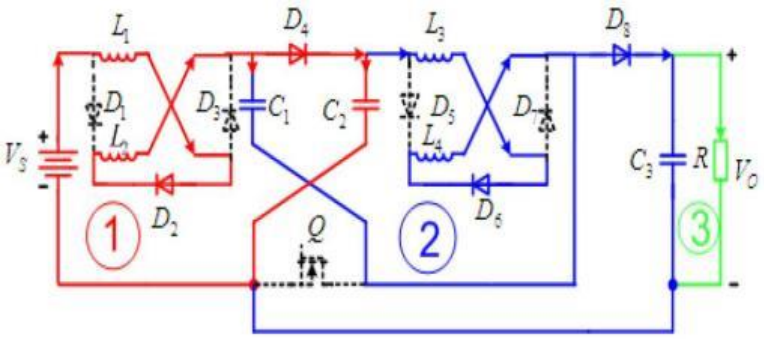

Figure.6. Equivalent circuit- Mode 2

Loop 2 is formed by Vs, L_1, D_2, L_2,D_4, L_3, D_6, L_4, D_8 and C_3, where Vs and L_1; :::;L_4 discharge energy to C_3 and Z_L, hence $V_s = v_{L1} + v_{L2} + v_{L3} + v_{L4} + V_{C3}$, and current i_{C3} decreases due to the discharge of energy to load Z_L. Meanwhile Loop 2 marked with blue line. The currents i_{L3} and i_{L4} decrease as shown in Figure. 6(c). The currents of D_6 and D_8 are equal to i_{L3} for the cascaded connection. Then, one has

$$\begin{cases} v_{L_3} + v_{L_4} = V_s - (v_{L_1} + v_{L_2} + V_{C_3}), \\ V_{C_1} = v_{L_3} + v_{L_4} = V_{C_2} - V_{C_3}. \end{cases}$$

According to this analysis, the output voltage Vo is derived as follows. Owing to the constance of the magnetic flux through an inductor, one has

$$\begin{cases} \int_0^{DT} (v_{L_1} + v_{L_2})\mathrm{d}t + \int_{DT}^{T} (v_{L_1} + v_{L_2})\mathrm{d}t = 0, \\ \int_0^{DT} (v_{L_3} + v_{L_4})\mathrm{d}t + \int_{DT}^{T} (v_{L_3} + v_{L_4})\mathrm{d}t = 0. \end{cases}$$

and a relationship between duty-cycle D and voltage gain M, namely,

$$V_o = V_{C_3} = V_s \frac{1+D}{1-3D},$$

$$V_{C_1} = -V_s \frac{2D}{1-3D},$$

$$V_{C_2} = V_s \frac{1-D}{1-3D}.$$

$$M = \frac{V_o}{V_s} = \frac{1+D}{1-3D},$$

can be obtained.

It is emphasized that the proposed converter can reach a much higher voltage gain than the conventional and the quadratic ones as well as the 3-Z-network boost converter with a small duty cycle D.

C) Waveforms of the proposed converter in CCM

In order to describe the operation process of the converter, its key waveforms in the steady state are shown in Figure 6, where Figure. 6(a) depicts the voltage vg driving switch Q. This rectangularly shaped gating signal has period T and duty-cycle D, i.e. it is on in every period for D*T time units. Fig. 6(b)shows the waveform of currents i_{L1} ; i_{L2} through L_1 and L_2, respectively, Fig. 6(c) the one of i_{L3} ; i_{L4} through L_3 and L_4, respectively. Fig. 6(d) presents the proposed converters output voltage.

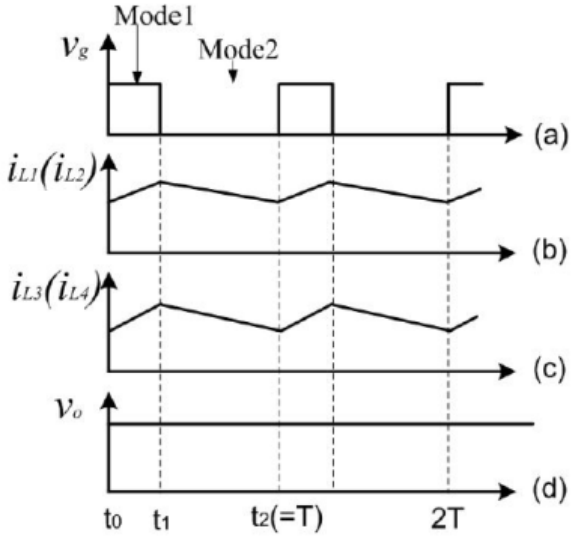

Figure .7. Key waveforms of the proposed converter in CCM: Subfigure (a) shows the voltage vg driving switch Q, (b) the waveforms of i_{L1} ; i_{L2} and (c) of i_{L3} ; i_{L4} , and (d) indicates the output voltage vo.

2) Converter-2 (3-Z-network boost converter with one diode and one capacitors in the middle link)

As Figure. 8(a) shows, there are two modes in this case, namely, Modes 1 and 2, whose equivalent circuits are shown in Figure. 8(a) and (b).

A) Mode 1: t - [t_0;t_1]

As shown in Figure. 8(a), there are three loops in the circuit, marked in different colors, and the arrows in the circuit refer to the current direction in each loop. As Q turns on, diodes D_1, D_3, and D_4 undertake positive voltages and turn on synchronously; meanwhile, D_2 bears negative voltage and turns off.

Thereafter, L_1 and L_2 are connected in parallel and then cascaded with D_4, Q, and V_s to form loop 1 with red lines. The source Vs discharges the energy to L_1 and L_2, then i_{L1} and i_{L2} increase, and L_1 and L_2 store the energy. The waveforms (blue lines) of i_{D1} , i_{D3} , i_{L1} , and i_{L2} are shown in Figure. 9(a)(2), where $i_{D1} = i_{D3} = i_{L1} = i_{L2}$; and i_{D4} , which is the current of D_4, endures $i_{L1} + i_{L2}$, namely, $i_{D4} = i_{L1} + i_{L2} = 2i_{L1}$. Meantime, D_5 and D_7 undertake negative voltages and turn off, yet D_6 and D_8 endure positive voltages and turn on. Accordingly, L_3 and L_4 are connected in parallel and then cascaded with Q and C_1 to form loop 2 in blue. C_1 discharges the energy to L_3 and L_4, and i_{L3} and i_{L4} increase. Thus, L_3 and L_4 store energy. The waveforms of i_{D6} , i_{D8} , i_{L3} , and i_{L4} are shown in blue in Figure. 9(a)(3), and the waveform of i_{C1} is shown in Figure. 9(a)(4), where $i_{D6} = i_{D8} = i_{L3} = i_{L4}$, and $i_{C1} = -2i_{L3}$, respectively. Meanwhile, D_9 endures the negative voltage and turns off, then the capacitor C_2 and the load R are cascaded to form loop 3 in green. Therein, C_2 discharges the energy to R, then the output voltage of the converter V_o reads

$$V_o = V_{C2}$$

where V_{C2} is the voltage of capacitor C_2.

B) Mode 2: t - [t_1;t_2]

At t_1, Q turns off, and the mode changes from Mode 1 to Mode 2, as shown in Figure. 8(b). As Q is off, D_1, D_3, D_4, D_6, and D_8 undertake negative voltage and turn off, yet D_2, D_5, D_7, and D_9 turn on and then form three loops in this mode. Therein, loop 1 is marked with red, namely, Vs–L_1–D_2–L_2–D_5–C_1, where Vs, L_1 and L_2 discharge energy to C_1, namely, $Vs = v_{L1} + v_{L2} + v_{C1}$. Moreover, i_{L1} and i_{L2} decrease as the red lines shown in Figure. 9(a)(2), and the currents of D_2 and D_5 are equal to i_{L1} for the cascaded connection, and i_{C1} increases as shown in Figure. 9(a)(4).

V_s, L_1, D_2, L_2, D_5, L_3, D_7, L_4, D_9, and C_2 form loop 2 marked with red and blue lines, where Vs, L_1, L_2, L_3, and L_4 discharge the energy to C_2 and R, namely, $Vs = v_{L1} + v_{L2} + v_{L3} + v_{L4} + v_{C2}$, and i_{C2} decreases due to the discharge energy to the load R. Moreover, i_{L3} and i_{L4} decrease as the red lines shown in Figure. 9(a)(3), and the currents of D_7 and D_9 are equal to i_{L3} for the cascaded connection.

$$i_{D7} = i_{D9} = i_{L3} = i_{L4}$$

$$i_{D6} = i_{D8} = 0$$

$$v_{L3} + v_{L4} = V_s - (v_{L1} + v_{L2} + v_{C2})$$

C) Waveforms of the proposed converter in CCM

Moreover, Figure. 9(a)(1) describes the driven voltage vg of switch Q; Figure. 9(a)(2) illustrates the waveform of i_{L1} (i_{L2}), which is composed of two parts with the blue one referring to the waveform of i_{D1}(= i_{D3}) and the red one to the waveforms of i_{D2}(= i_{D5}); Figure. 9(a)(3) depicts the waveform of i_{L3} (i_{L4}), which is also composed of two parts with the blue one referring to the waveform of i_{D6}(= i_{D8}) and the red one to the waveform of i_{D7}(= i_{D9}); and Figure. 9(a)(4) portrays the waveforms of i_{C1} . Therein, i_{L1} , i_{L2} , i_{L3} , i_{L4} , i_{D1} , i_{D2} , i_{D3} , i_{D5} , i_{D6} , i_{D7} , i_{D8} , i_{D9} , i_{C1} , and i_{C2} are the currents of L_1, L_2, L_3, L_4, D_1, D_2, D_3, D_5, D_6, D_7, D_8, D_9, C_1, and C_2, respectively.

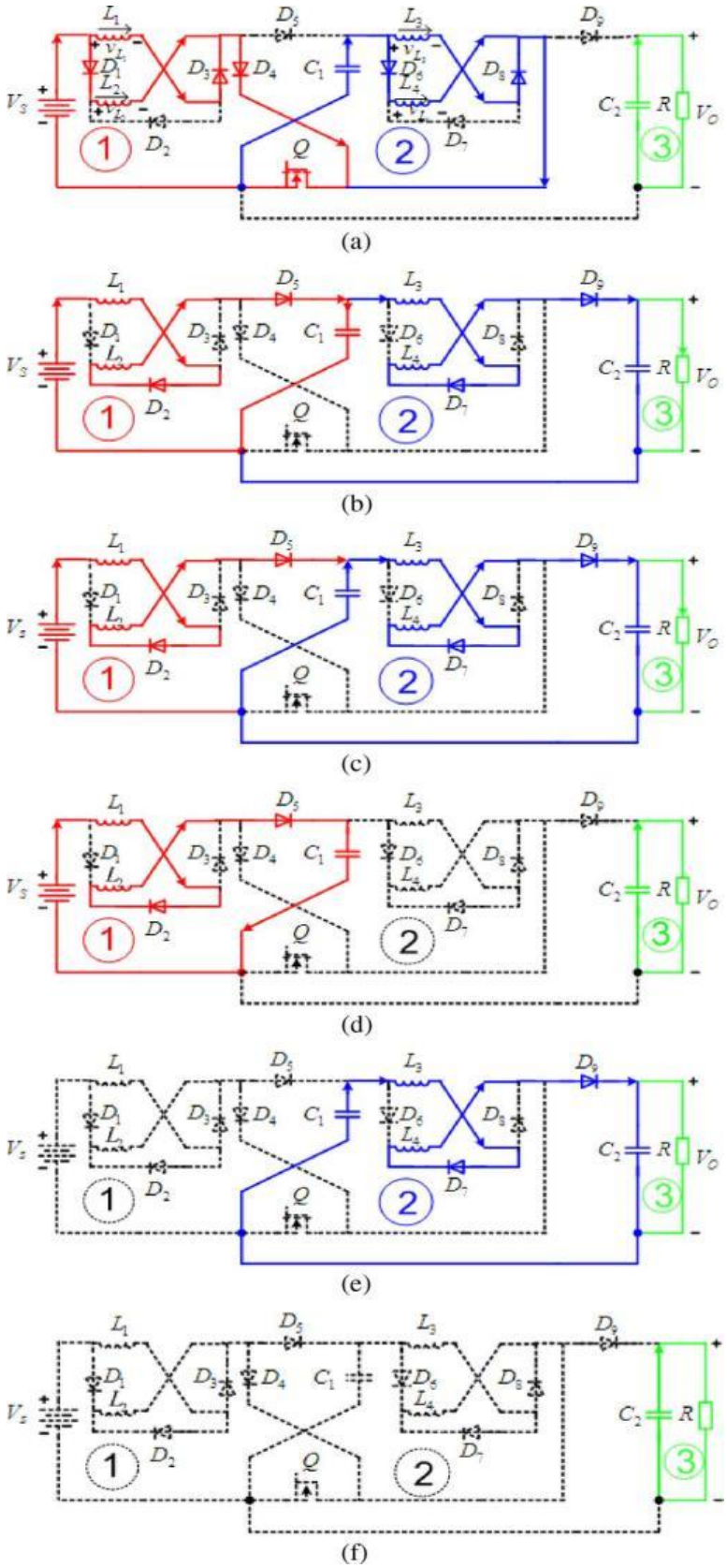

Figure. 8. Equivalent circuits. (a) Mode 1: Q, D_1, D_3, D_4, D_6, and D_8 on, D_2, D_5, D_7, and D_9 off. (b)Mode 2: D_2, D_5 D_7, and D_9 on, Q, D_1, D_3, D_4, D_6, and D_8 off. (c) Mode 3: D_2, D_5, D_7, and D_9 on, Q, D_1, D_3, D_4, D_6, and D_8 off. (d) Mode 4: D_2, D_7, and D_9 on, Q, D_1, D_3, D_4, D_5, D_6, D_7, and D_8 off. (e) Mode 5: D_2 and D_5 on, Q, D_1, D_3, D_4, D_6, D_7, D_8, and D_9 off. (f) Mode 6: Q, D_1, D_2, D_3, D_4, D_5, D_6, D_7, D_8, and D_9 off.

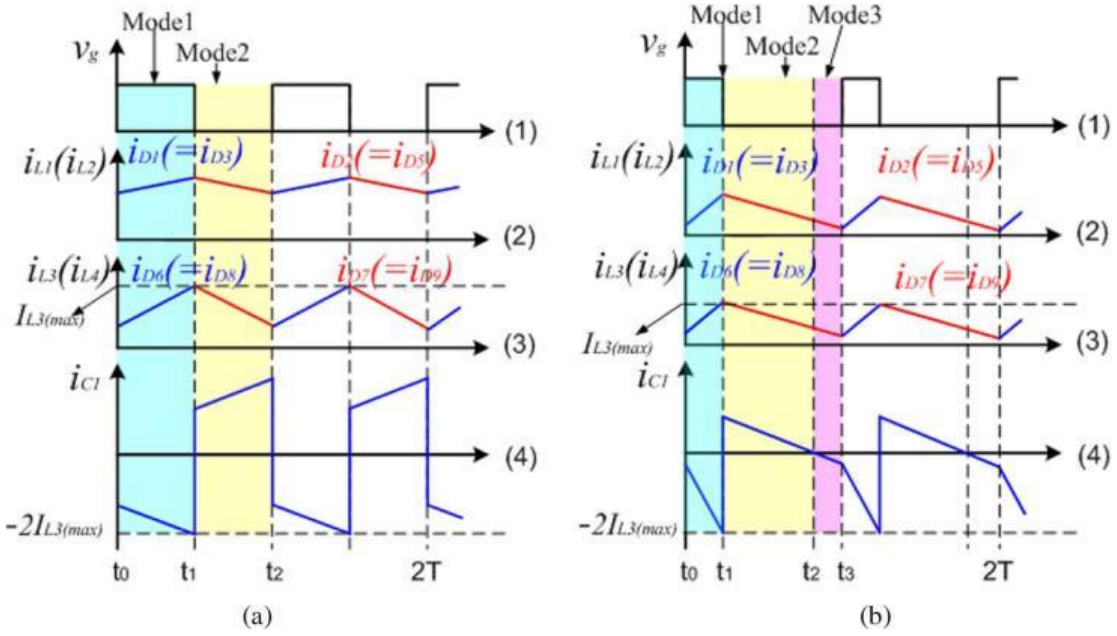

Figure. 9. Key waveforms of the 3-Z-network boost converter in CCM. (a) Case 1. (b) Case 2. In each subfigure, (1) describes the driven voltage vg of switch Q; (2) illustrates the waveform of i_{L1} (i_{L2}), composed of two parts with the blue one referring to the waveform of i_{D1}(= i_{D3}) and the red one to the waveform of i_{D2}(= i_{D5}); (3) depicts the waveform of i_{L3} (i_{L4}), composed of two parts with the blue one referring to the waveform of i_{D6}(= i_{D8}) and the red one to the waveform of i_{D7}(= i_{D9}); and (4) portrays the waveform of i_{C1}.

V. OUTPUT VOLTAGE AND VOLTAGE STRESS OF COMPONENTS IN VARIOUS CONVERTERS

According to the analyses of Cases 1 and 2, the output voltage Vo is deduced as follows. In terms of the voltage second constant theory, one has

$$V_o = V_{C_2} = V_s \left(\frac{1+D}{1-D}\right)^2$$

$$V_{C_1} = V_s \frac{1+D}{1-D}.$$

one can obtain the output voltage V_{op} as,

$$V_{op} = \left((V_s - 2V_D)\left(\frac{1+D}{1-D}\right) - 2V_D\right)\left(\frac{1+D}{1-D}\right)$$

where V_D is the voltage of the diodes. The relationships of duty cycle D and voltage gain M = Vo/Vs in conventional boost converters, quadratic boost converters, and 3-Znetwork boost converters are depicted in Figure.10 in different colours, respectively, with a zoom-in for 0 < D <0.5. It is remarked that the proposed converter can reach a much higher voltage gain than the quadratic and the conventional ones. There in, V_{L1} , V_{L2} , V_{L3} , and V_{L4} refer to the average voltages of L_1, L_2, L_3, and L_4 when Q is ON and OFF, respectively. Thus,

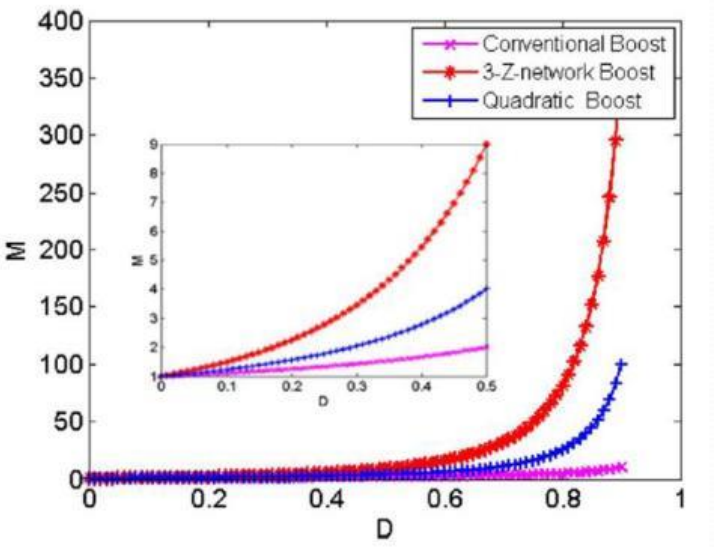

Figure.10. Relationship figure of duty cycle D and voltage gain M

In terms of Kirchhoff's voltage law, one can obtain the voltage of each component in the circuit as shown in TABLE I.

Parameter / Type	V_Q	I_Q	V_D	I_D
Conventional	$V_s\frac{1}{1-D}$	$I_o\frac{1}{1-D}$	$V_s\frac{1}{1-D}$	$I_o\frac{1}{1-D}$
Quadratic	$V_s\frac{1}{(1-D)^2}$	$I_o\frac{1}{(1-D)^2}$	$V_s\frac{1}{(1-D)^2}$	$I_o\frac{1}{(1-D)^2}$
3-Z-network	$V_s\frac{(1+D)^2}{(1-D)^2}$	$I_o\frac{4D}{(1-D)^2}$	$V_s\frac{(1+D)^2}{(1-D)^2}$	$I_o\frac{2D}{(1-D)^2}$
Proposed	$V_s\frac{1+D}{1-3D}$	$I_o\frac{4D(1-2D)}{(1+D)^2}$	$V_s\frac{1+D}{1-3D}$	$I_o\frac{D(1-3D)}{(1+D)^2}$

A comparison of number of switches and diodes, and voltage gain of each converter is given in TABLE III

TABLE 111

Parameter / Type	Switch	Diode	M
Conventional	1	1	$\frac{1}{1-D}$
Quadratic	2	2	$\frac{1}{(1-D)^2}$
3-Z-network	1	9	$\frac{(1+D)^2}{(1-D)^2}$
Proposed	1	8	$\frac{1+D}{1-3D}$

$$V_{L_1} = V_{L_2} = \begin{cases} V_s, & \text{if } Q \text{ is on} \\ -V_s \frac{D}{1-D}, & \text{otherwise} \end{cases}$$

$$V_{L_3} = V_{L_4} = \begin{cases} V_s \frac{1+D}{1-D}, & \text{if } Q \text{ is on} \\ -V_s \frac{D(1+D)}{(1-D)^2}, & \text{otherwise.} \end{cases}$$

Assuming a lossless circuit leads to $V_s\ I_{in} = V_o\ I_o$, where I_{in} and I_o are input and output currents, respectively.

$$I_{\text{in}} = I_o \frac{(1+D)^2}{(1-D)^2}.$$

and Similarly ,I_{L1} , I_{L2} , I_{L3} and I_{L4} can be expressed as,

$$I_{L_1} = I_{L_2} = I_o \frac{1+D}{(1-D)^2}.$$

$$I_{L_3} = I_{L_4} = I_o \frac{1}{1-D}.$$

VI. SIMULATION RESULTS

To verify the feasibility and validity of the proposed converter, MATLAB software is used for the simulation.

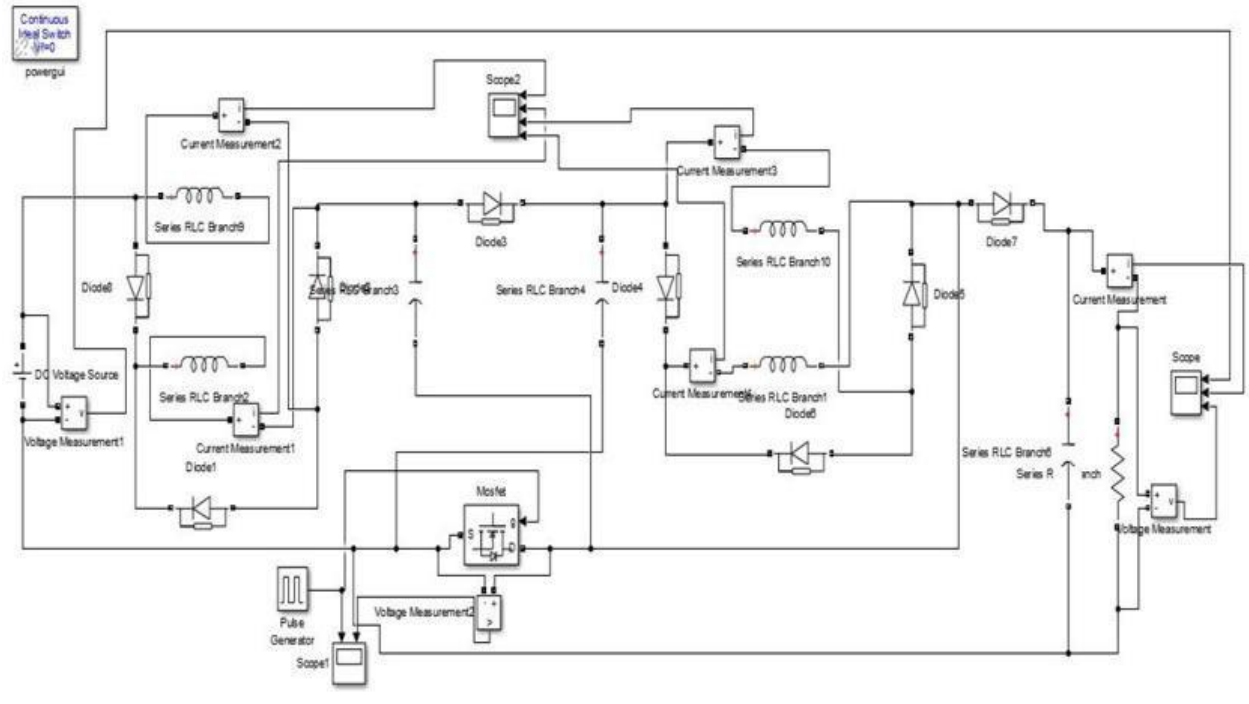

Figure.11. Simulation diagram 3-Z-network boost converter.

Let the parameters V_s= 20 V and T = 10 uS be preassigned, and assume the converter parameters as $C_1 = C_2$ = 220 uF, C_3 = 470 uF, $L_1 = L_2$ = 100 uH and $L_3 = L_4$ = 200 uH. The graphs present the results of simulations carried out for D = 0.3 respectively. Figure.12. shows that show the output voltage V_0 and output current.

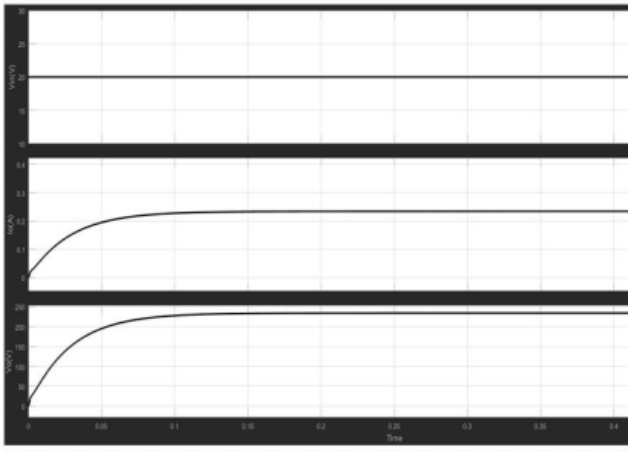

Figure.12. Output voltage and output current of 3-Z-network boost converter

Figure .13. shows the Waveform of switching pulse in detail. First graph is the voltage between the collector and emitter of the MOSFET.

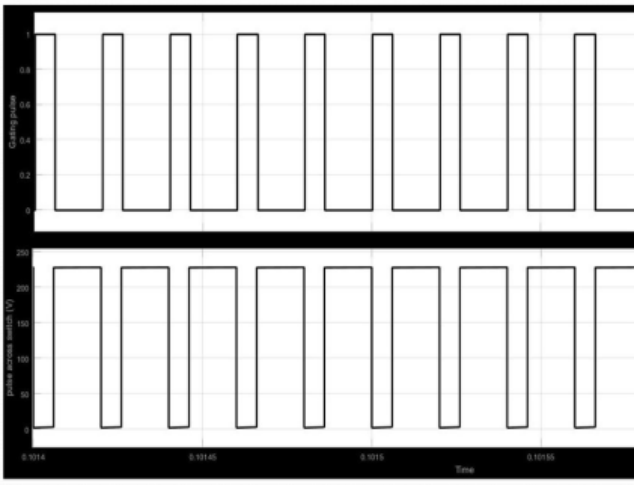

Figure.13. Gating pulse and voltage across switch of 3-Z-network boost converter

Figure.14. shows the currents through the inductors $L_1(L_2)$ and $L_3(L_4)$ respectively. It is obvious that the simulation results are consistent with the analysis above.

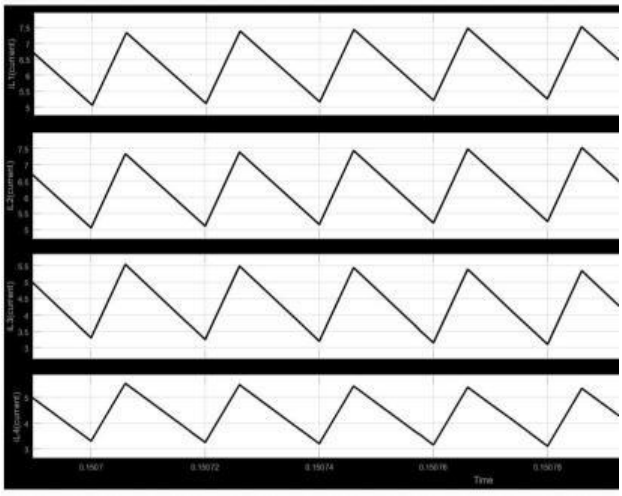

Figure.14. Charging and discharging of the inductor

VII. EXPERIMENTAL RESULTS

The results verifies that the proposed converter can generate a high voltage gain for solar energy systems to boost up the low voltage to the desired voltage. In our prototype for a input voltage 20 V and the duty cycle D = 0.3, the experimental waveforms shown in Figure.17 were generated by a 250W prototype. From top to bottom the current i_{L3} through L_3 (label 4), the voltages V_{C2} at C_2 (label 3), the output voltage V_o (label 2), and the drain-source voltage V_{DS} of switch Q (label 1), respectively, are provided in the Figure.14 that the output voltage is about 215 V, which is reasonable due to the diode drops in the proposed converter, and the results also verify that the proposed converter can generate a high voltage gain for solar energy systems to boost up the low voltage to the desired voltage.
Considering the voltage drops at the switch and diodes, the efficiency of the converter can be described by,

$$\eta = \frac{P_{out}}{P_{in}} = \left[\frac{V_s(1+D) - 4DV_Q - 4V_D}{V_s(1+D)}\right]^2$$

where Pout, Pin, V_Q and V_D are the output power, the input power, and the voltage at switch and diodes (assuming the same voltage V_D at all diodes), respectively. Since there is one less diode compared to the traditional one, the efficiency is higher . With D = 0.3, $V_Q = V_D$ = 1.2V and Vs = 20V , the efficiency of the converter is about 92.6 percentage, while the measured one reaches 90.5 percentage, which is higher than the traditional one both in theory analysis and experiments.

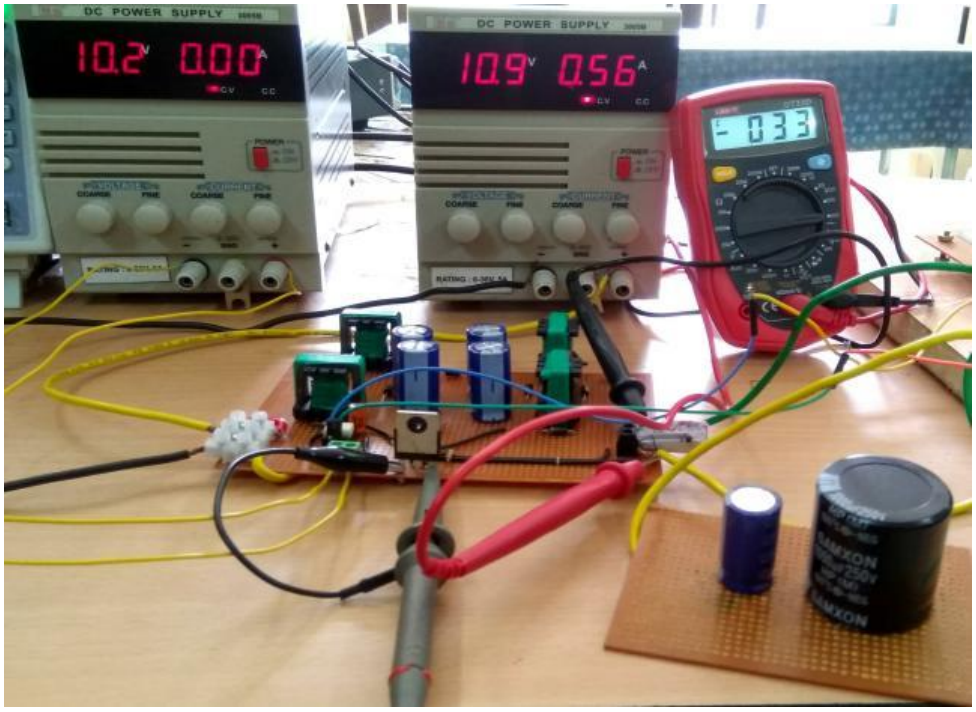

Figure.15. Prototype of the proposed converter.

The experimental setup and experimental waveforms are shown in Figure.16 and Figure.17 were generated by a 250W prototype. From top to bottom the current i_{L3} through L_3 (label 4), the voltages v_{C2} at C_2 (label 3), the output voltage Vo (label 2), and the drain-source voltage V_{DS} of switch Q (label 1), respectively, are provided in the Figure.17.

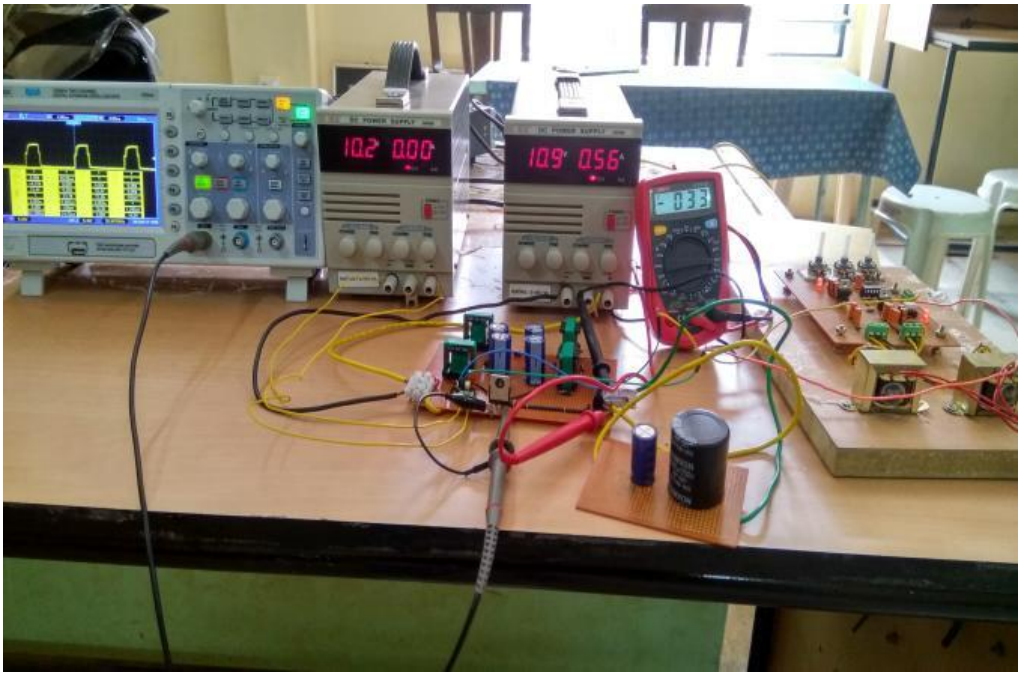

Figure.16. Experimental setup of the proposed converter.

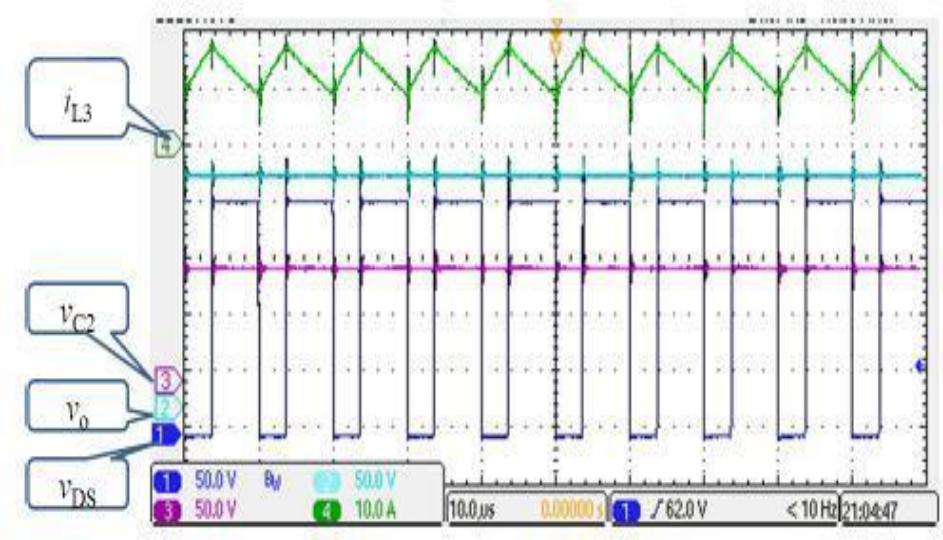

Figure.17. Experimental waveforms with D = 0.3

VIII. CONCLUSION

High-step-up and high-efficiency DC-DC converters are necessary to handle large input currents and to reach high output voltages, e.g. where the low voltages of renewable energy sources need to be boosted to high voltages for feeding into grid-connected inverters. Theoretically, conventional boost converters may realize infinite voltage gains for switching duty-cycles very close to 100 percentage which, however, degrade the converters overall efficiency. This drawback is overcome by the proposed high-step-up boost converter-1. A comparison among the conventional boost converter, the quadratic one, the 3-Z-network converter and the proposed converter is conducted in this paper. With the same D ranges within [0; 1/3), it is obvious that the proposed one, compared to the other three boost converters, has higher voltage gain, lower current stresses but higher voltage stresses on switches and diodes.

Moreover, 3-Z-network converter (converter-2) reaches a voltage gain by a large D which results in the saturation of inductors, while the converter-1 can avoid this since D ranges within [0; 1/3). One can also obtain that the converter-1 an achieve lower voltage stress than one of 3-Z-network within a same voltage gain. Hence, the converter-1 as better features than 3-Z-network converter. By suitably adjusting the duty-cycle, desired voltage gain in renewable energy systems can be achieved. A detailed operational analysis of the converter was given and validated by simulations and experiments with a 250W prototype built. They all prove the effective comparison of the proposed converter.

REFERENCES

[1] Guidong Zhang, Herbert Ho-Ching Iu, Bo Zhang,Zhong Li, Tyrone Fernando, Si- Zhe Chen, and Yun Zhang,An Impedance Networks Boost Converter with Highvoltage Gain , IEEE Trans. Power Electron., DOI 10.1109/TPEL.2017.2673545.

[2] J.C. Hui, A. Bakhshai, and P.K.Jain, An energy management scheme with power limit capability and an adaptive maximum power point tracking for small standalone pmsg wind energy systems, IEEE Trans. Power Electron., Vol. 31, No. 7, pp. 48614875, Jul., 2016.

[3] L. Zhang, K. Sun, Y. Xing, and J. Zhao, A family of five-level dual buck full-bridge inverters for grid-tied applications, IEEE Trans. Power Electron., Vol. 31, No. 10, pp. 70297042, Oct., 2016.

[4] A. Calle-Prado, S. Alepuz, J. Bordonau, J. Nicolas-Apruzzese, P. Cortes, and J. Rodriguez, Model predictive current control of grid-connected neutral-point-clamped converters to meet low-voltage ride-through requirements, IEEE Trans. Ind. Electron., Vol. 62, No. 3, pp. 15031514, Mar., 2015.

[5] H.L. Ginn and G. Chen, Digital control method for grid-connected converters supplied with nonideal voltage, IEEE Trans. Ind. Inf., Vol. 10, No. 1, pp. 127136, 2014.

[6] X. G. Feng, J. J. Liu, and F. C. Lee, Impedance specifications for stable DC distributed power systems, IEEE Trans. Power Electron., vol. 17, no. 2, pp. 157162, Mar. 2002.

[7] M.A. Al-Saffar, E.H. Ismail and A.J. Sabzali, Family of ZC-ZVS converters with wide voltage range for renewable energy systems, Renew. Energ., Vol. 56, pp. 3243, Aug., 2013.

[8] Ahmad J. Sabzali, Esam H. Ismail, Hussain M. Behbehani, High voltage step-up integrated double BoostCSepic DCCDC converter for fuel-cell and photovoltaic applications, Renew. Energ., Vol. 82, pp. 44 53, Oct., 2015.

[9] C. Mario, C. Alfio, A. Rosario and G. Francesco, Soft-switching converter with HF transformer for grid-connected photovoltaic systems, IEEE Trans. Ind. Electron., Vol. 57, No. 5, pp. 16781686, May, 2010.

[10] W. Li, Y. He, X. He, Y. Sun, F. Wang and L. Ma, Series asymmetrical halfbridge converters with voltage autobalance for high input-voltage applications, IEEE Trans. Power Electron., Vol. 28, No. 8, pp. 3665 3674, Aug., 2013.

[11] K.I. Hwu, C.F. Chuang and W.C. Tu, High voltage-boosting converters based on bootstrap capacitors and boost inductors, IEEE Trans. Ind. Electron., Vol. 60, No. 6, pp. 21782193, Jun., 2013.

[12] S. Vighetti, J.P. Ferrieux and Y. Lembeye, Optimization and design of a cascaded DC-DC converter devoted to grid-connected photovoltaic systems, IEEE Trans. Power Electron., Vol. 27, No. 4, pp. 20182027, Apr., 2012.